Correlation between lithium storage and diffusion properties and electrochromic characteristics of WO_3 thin films*

Yu Peng-Fei(于鹏飞), Cui Zhong-Hui(崔忠慧), Fan Wu-Gang(范武刚), and Guo Xiang-Xin(郭向欣)†

State Key Laboratory of High Performance Ceramics and Superfine Microstructure, Shanghai Institute of Ceramics, Chinese Academy of Sciences, Shanghai 200050, *China*

(Received 11 June 2012; revised manuscript received 18 August 2012)

As essential electrochromic (EC) materials are related to energy savings in fenestration technology, tungsten oxide (WO_3) films have been intensively studied recently. In order to achieve better understanding of the mechanism of EC properties, and thus facilitate optimization of device performance, clarification of the correlation between cation storage and transfer properties and the coloration performance is needed. In this study, transparent polycrystalline and amorphous WO_3 thin films were deposited on SnO_2:F-coated glass substrates by the pulsed laser deposition technique. Investigation into optical transmittance in a wavelength range of 400–800 nm measured at a current density of 130 $\mu A \cdot cm^{-2}$ with the applied potential ranging from 3.2 to 2.2 V indicates that polycrystalline films have a larger optical modulation of $\sim$ 30% at 600 nm and a larger coloration switch time of 95 s in the whole wavelength range compared with amorphous films ($\sim$ 24% and 50 s). Meanwhile, under the same conditions, polycrystalline films show a larger lithium storage capacity corresponding to a Li/W ratio of 0.5, a smaller lithium diffusion coefficient (2×10^{-12} $cm^2 \cdot s^{-1}$ for Li/W=0.24) compared with the amorphous ones, which have a Li/W ratio of 0.29 and a coefficient of $\sim 2.5\times10^{-11}$ $cm^2 \cdot s^{-1}$ as Li/W=0.24. These results demonstrate that the large optical modulation relates to the large lithium storage capacity, and the fast coloration transition is associated with fast lithium diffusion.

Keywords: WO_3 thin films, electrochromic material, lithium storage and diffusion

PACS: 81.15.Fg, 78.20.−e, 66.30.−h **DOI:** 10.1088/1674-1056/22/3/038101

1. Introduction

Electrochromic (EC) materials can change the optical absorption in a broad visible range as charged ions, such as H^+ or Li^+, are electrochemically inserted or extracted.[1] They have attracted much attention in both applied and fundamental research in the past several decades.[2–9] Recently, the application of "smart windows" related to energy saving and indoor comfort have stimulated new interests for high-performance EC films combined with fenestration technology.[10–14] In this context, tungsten oxide (WO_3) films are attractive, not only because they are used in most oxide-based EC devices, but also because many fundamental issues related to the charge-injection induced coloration are not completely clear.[15–25]

In previous reports, there are numerous discussions on the factors which have a significant influence on the EC performance of WO_3 films. Niklasson *et al*.[10] reported that the WO_3 films grown by the sputtering have to be amorphous for high EC performance, because the polycrystalline films only have sufficient optical modulation in the near-infrared spectral region. Bathe *et al*.[25] stated that polycrystalline films prepared by using a pulsed spray pyrolysis deposition technique show a better EC performance than amorphous films. It is worth noting that these discussions were focused on the crystallinity effect on the EC performance. Difference in film microstructure produced with different growth techniques was not taken into account. It is well known that different microstructures with different particle size and pore structure may greatly affect the electron transfer and ion diffusion in host materials,[26] causing a large difference in the EC property.[27,28] In addition, defects such as oxygen vacancies or interstitials are found to be the causes of different transport[29] and EC properties in different research studies.[30] As a result, many factors including crystallinity, microstructure and chemical defects should be taken into account for understanding the origins of different electrochromic behaviours. As the coloration process of WO_3 involves injections and extractions of cations and electrons simultaneously,[3,31] cation diffusion and storage properties that are closely related to the crystal structure, microstructure and point defects are expected to have a great influence on the EC characteristics. In this study, lithium storage and transport properties of amorphous and polycrystalline WO_3 thin films in combination with the EC characteristics were investigated. It proves that the investigation of lithium storage and diffusion properties in the films facilitates the interpretation of different EC behaviours.

2. Experimental setup

The WO_3 thin films were prepared by PLD in a high vacuum chamber with a base pressure of 2×10^{-4} Pa. During deposition, laser beams from a XeCl excimer laser (COMP-

*Project supported by the National Natural Science Foundation of China (Grant No. 10979069) and the "Hundred Talent Program" of Chinese Academy of Sciences.

†Corresponding author. E-mail: XXGuo@mail.sic.ac.cn

© 2013 Chinese Physical Society and IOP Publishing Ltd

exPro201, Germany) with a wavelength of 308 nm, pulse duration of 25 ns, and repetition rate of 2 Hz were focused on a rotating WO_3 ceramic target with an incident angle of 45°. The targets with a diameter of 32 mm were fabricated by sintering powders at 1000 °C for 24 h in air. The energy density of the focused laser beam was fixed at $\sim 8\ \mathrm{J\cdot cm^{-2}}$. Substrates of SnO_2:F (FTO)-coated glasses were mounted on the holder and rotated during deposition. The distance between the target and the substrate was 7.5 cm. The films were grown at a substrate temperature of 200 °C or 400 °C and a oxygen pressure of 14 Pa. The growth temperature was detected by a thermal couple attached to the backside of the sample holder.

Crystallinity of the samples was analyzed by a thin-film X-ray diffractometer (XRD, D8 Discover, Bruker) in the range of 20°–75° at a scanning rate of 0.02°/s using Cu K_α radiation. Scanning electron microscopy (SEM, Hitachi S-4800) was carried out to investigate the surface and cross-section morphologies of the films.

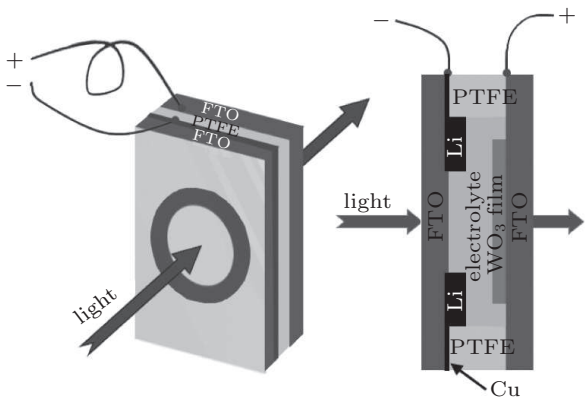


Fig. 1. Schematic diagram for the electrochemical cell which allows optical transmittance measurement during Li^+ insertion/extraction cycles. FTO represents SnO_2:F glass, PTFE represents polytetrafluoroethylene.

Optical transmittance of the films during Li insertion and extraction cycles was characterized by using the electrochemical cells, as shown in Fig. 1. The cell includes an FTO glass substrate coated by a WO_3 layer and a 0.15-mm-thick Li foil with a hole of diameter of 1 cm as counter electrode, which is connected with a Cu current collector to avoid a reaction of Li^+ with the FTO. A space between the above parts was obtained by the groove of polytetrafluoroethylene (PTFE) which was filled by 1M $LiPF_6$ dissolved in ethylene carbonate (EC) and dimethyl carbonate (DMC) at a volume ratio of 1:1 (Ferro Corporation, USA). Every cell was assembled in an argon-filled glove box with oxygen and moisture levels below 1 ppm. It was sealed by an epoxy resin to prohibit air invasion after moving out of the glove box. Using these cells, the optical transmittances were recorded by a UV-visible spectrophotometer (Hitachi U-4100) during the charge-discharge processes using an automatic battery tester (Land CT-2001A). The electrochemical impedance spectroscopy (EIS) measurements were carried out in glass cells with the separated lithium foil as the reference electrode using a workstation (Autolab) with a frequency response analyzer ranging from 10 kHz to 0.01 Hz.

3. Results and discussion

As can be seen in Fig. 2, the WO_3 thin films deposited at 200 °C show no peaks in the XRD curve, indicating an amorphous structure. In contrast, the films deposited at 400 °C clearly show peaks corresponding to the polycrystalline WO_3 (JCPDS 20-1324). This result is consistent with previous studies which indicated that the crystallization of evaporated amorphous WO_3 films in general occurred at 370 °C–400 °C.[32,33]

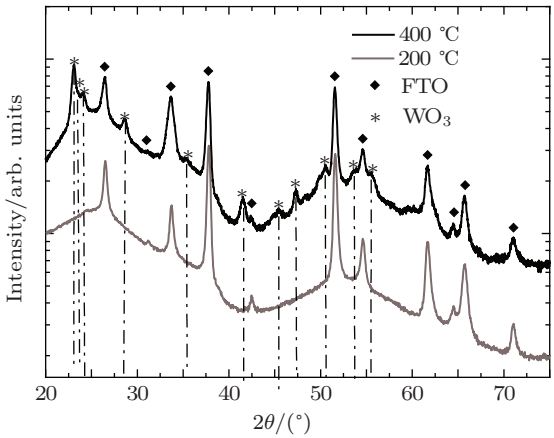


Fig. 2. X-ray diffraction (XRD) scans for the WO_3 thin films grown on FTO-coated glass substrates at deposition temperatures of 200 °C and 400 °C. The XRD peaks from the substrate are also shown for comparison. The dash-dotted lines denote the peak positions corresponding to WO_3 (JCPDS 20-1324).

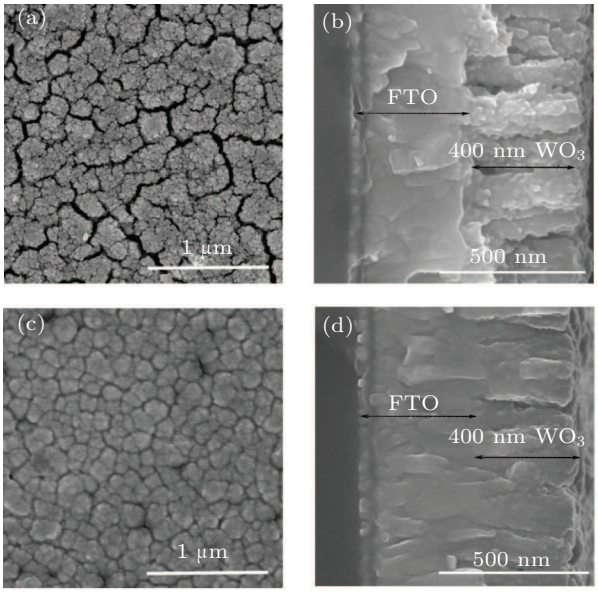


Fig. 3. Scanning electron microscope (SEM) images for the WO_3 thin films grown on the FTO-coated substrates at different substrate temperatures. (a) Surface and (b) cross-section morphology images for the grown film at 200 °C and (c, d) at 400 °C.

Surface and cross-section morphologies of the films were investigated by SEM, which are shown in Figs. 3(a)–3(d). For the two-kind films, approximately the same thickness of 400 nm is revealed by the cross-section images displayed in Figs. 3(b) and 3(d). In these figures, it can also be clearly observed that both films consist of similar column-like particles perpendicular to the substrate. The film grown at 200 °C has smaller particles and more pores than at 400 °C. Thus, the XRD and the SEM results reveal that the elevated growth temperature leads to a denser film with larger particles and less pores.

The transmittance spectra of the amorphous and the polycrystalline films in the range of 400–1000 nm were studied by a UV–visible spectrophotometer. The spectra for both kinds of films at the bleached state (3.2 V) and the colored state (2.2 V) are shown in Fig. 4 with the subtracting background of FTO glasses. It can be seen that the optical modulation of polycrystalline WO_3 films is much larger than that of the amorphous WO_3 films.

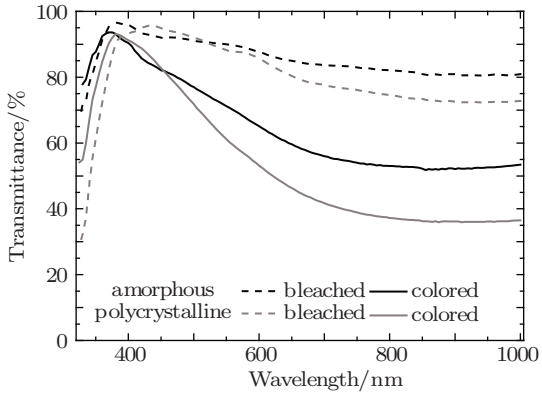


Fig. 4. Transmittance spectra of amorphous and polycrystalline WO_3 with the removal of the background of FTO glasses at bleached and colored states, respectively, measured at the current density of 130 μA/cm^2. The applied potential ranges from 3.2 to 2.2 V.

The *in situ* optical transmittance at a wavelength of 600 nm for the amorphous and the polycrystalline films were investigated by the electrochemical cells shown in Fig. 1 during the lithiation and delithiation processes at the same current density (130 μA·cm^{-2}) as well as the same potential range (2.2–3.2 V) applied during the discharge and charge processes, which is shown in Fig. 5. The polycrystalline and amorphous films exhibit an optical modulation of ∼ 30% and 24%, which is in accordance with the results shown in Fig. 4. The switching time between the maximum and the minimum transmittance is much longer for the polycrystalline film (95 s) than for the amorphous one (50 s).

These different EC behaviors may be closely related to the lithium diffusion and storage properties. Figure 6 shows the discharge/charge curves for the two-kind films recorded during the *in situ* optical transmittance measurement at the current density of 130 μA·cm^{-2} and the potential range of 2.2–3.2 V. Such curves were reproducible over 200 cycles in experiment. As can be seen in the figure, the polycrystalline film can store a larger amount of lithium than the amorphous one. Under the same discharge/charge conditions, the lithium/tungsten ratio for the polycrystalline film can be as large as ∼ 0.50, while that for the amorphous film is ∼ 0.29. This result indicates that larger optical modulation of the polycrystalline film correlates well with the larger lithium storage capacity.

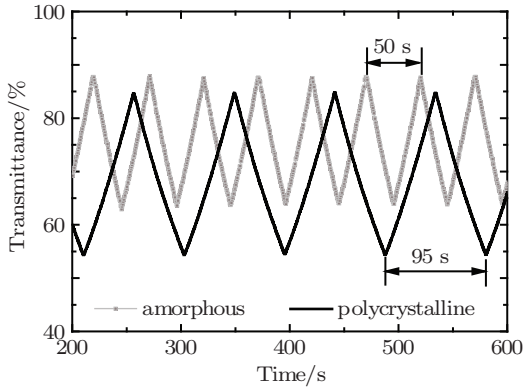


Fig. 5. Transmittance at the optical wavelength of 600 nm for the amorphous and the polycrystalline WO_3 films, measured in the cell shown in Fig. 1 during the lithiation and delithiation processes at a current density of 130 μA/cm^2 in the same applied potential range (2.2–3.2 V).

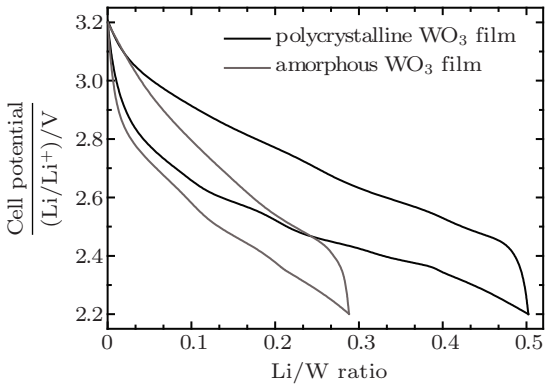


Fig. 6. Discharge and charge curves measured during the optical transmittance detection for the two-type films.

The electrochemical impedance spectroscopy (EIS) measurements for each cell were carried out on the same samples as the EC characterizations. Each EIS was recorded after being discharged to a specific potential and reaching equilibrium. Typical profiles of the spectra can be seen in Fig. 7. It can be seen that each EIS consists of three sections. From the high to low frequency, section (i) is an intersection on the real impedance axis, which can be attributed to the electronic conduction through the current collectors or electrodes and ionic conduction through the liquid electrolyte. Section (ii) consists

of two semicircles. In Ref. [34], the first semicircle was attributed to the electron injection at the electrode/WO_3 interface. The second one was due to the injection of Li^+ into the bulk part of the WO_3 film. Section (iii) exhibits typical Warburg behavior, which can be attributed to the diffusion of Li^+ into the bulk of WO_3.[35] Based on section (iii), the diffusion coefficient of lithium can be calculated by

$$\tilde{D}_{\mathrm{Li}} = \frac{1}{2}\left[\left(\frac{V_{\mathrm{m}}}{FS\sigma}\right)\left(\frac{\mathrm{d}E}{\mathrm{d}x}\right)\right]^2, \qquad (1)$$

where V_{m} stands for the molar volume, S means the surface area of the electrode, F is the Faraday constant, $\mathrm{d}E/\mathrm{d}x$ is the differential of the electrode potential E with respect to composition x, and σ is the Warburg factor which can be obtained by the slope of Z_{Re} or $-Z_{\mathrm{Im}}$ versus $\omega^{-1/2}$.

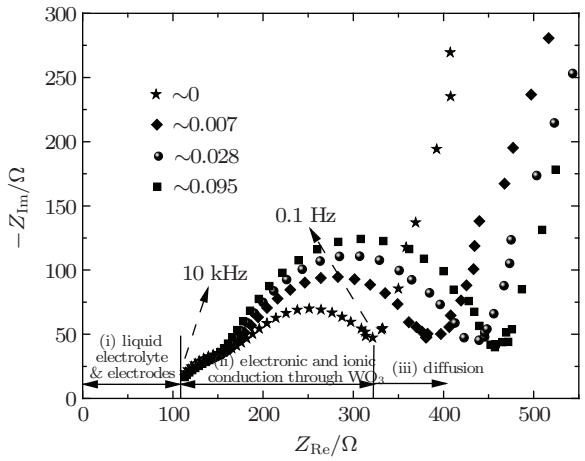


Fig. 7. Electrochemical impedance spectroscopy (EIS) measurements for the amorphous films with Li^+ intercalated with different Li/W ratios.

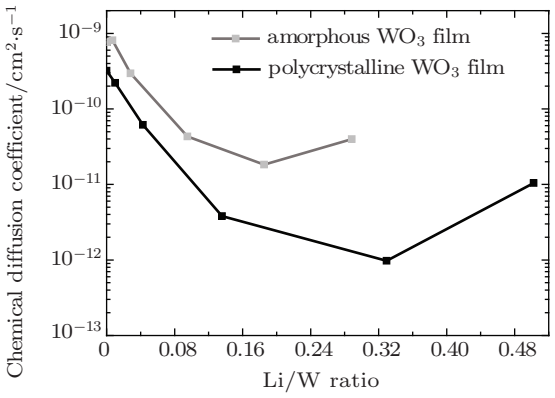


Fig. 8. Chemical diffusion coefficient versus Li/W ratio for the polycrystalline and amorphous films.

The calculated diffusion coefficients of lithium in the two-kind films are displayed in Fig. 8. It is clear that in the investigated Li/W ratio range, the chemical diffusion coefficients of lithium for the amorphous film are greater than for the polycrystalline film. As discussed above, the coloration transition for the amorphous film is faster than for the polycrystalline one. In combination with the above storage properties, we can draw the conclusion that the polycrystalline films have larger lithium storage capacities and the smaller lithium diffusion coefficients than the amorphous ones, leading to the larger optical modulation and the slower coloration transition. This result is reasonable given that the larger lithium storage corresponds to the greater amount of electron injection/extraction into/from the host material, and thus is a more obvious influence on the optical absorption. The larger lithium diffusion coefficient means a faster movement of lithium, leading to a smaller switch time between the colored and bleached states.

4. Conclusion

In summary, the EC characteristics and the electrochemical properties of the polycrystalline and the amorphous WO_3 thin films are comparatively studied. The former films exhibit larger optical modulations and slower coloration responses than the latter ones. These different EC behaviors are found to be correlated with the lithium storage and diffusion properties. A larger lithium storage capacity together with a smaller lithium diffusion coefficient leads to a larger optical modulation but a slower color transition process in the case of the polycrystalline films. These results indicate that the EC performance can be effectively evaluated through electrochemical investigation of lithium transfer properties in the EC materials.

References

[1] Deb S K 1973 *Philos. Mag.* **27** 801
[2] Deb S K 1969 *Appl. Opt.* **8** 192
[3] Faughnan B W, Crandall R S and Heyman P M 1975 *Rca Rev.* **36** 177
[4] Somani P R and Radhakrishnan S 2003 *Mater. Chem. Phys.* **77** 117
[5] Granqvist C G 2000 *Sol. Energy Mater. Sol. Cells* **60** 201
[6] Granqvist C G, Avendaño E and Azens A 2003 *Thin Solid Films* **442** 201
[7] Granqvist C G 1994 *Sol. Energy Mater. Sol. Cells* **32** 369
[8] Granqvist C G 1995 *Handbook of Inorganic Electrochromic Materials* (Amsterdam: Elsevier)
[9] Granqvist C G, Azens A, Isidorsson J, Kharrazi M, Kullman L, Lindstrom T, Niklasson G A, Ribbing C G, Ronnow D, Mattsson M S and Veszelei M 1997 *J. Non-Cryst. Solids* **218** 273
[10] Niklasson G A and Granqvist C G 2007 *J. Mater. Chem.* **17** 127
[11] Baetens R, Jelle B P and Gustavsen A 2010 *Sol. Energy Mater. Sol. Cells* **94** 87
[12] Yu X Q, Wang R I, He Y, Hu Y S, Li H and Huang X J 2010 *Electrochem. Solid-State Lett.* **13** J99
[13] Ghodsi F E, Tepehan F Z and Tepehan G G 2008 *Sol. Energy Mater. Sol. Cells* **92** 234
[14] Svensson J S E M and Granqvist C G 1985 *Sol. Energ. Mater.* **12** 391
[15] Huang R, Zhu J and Yu R 2009 *Chin. Phys. B* **18** 3024
[16] Yuan H J, Chen Y Q, Yu F, Peng Y H, He X W, Zhao D and Tang D S 2011 *Chin. Phys. B* **20** 036103
[17] Vemuri R S, Bharathi K K, Gullapalli S K and Ramana C V 2010 *ACS Appl. Mater. Inter.* **2** 2623
[18] Kalantar-Zadeh K, Vijayaraghavan A, Ham M H, Zheng H, Breedon M and Strano M S 2010 *Chem. Mater.* **22** 5660
[19] Hu M, Zhang J, Wang W D and Qin Y X 2011 *Chin. Phys. B* **20** 082101

[20] Gullapalli S K, Vemuri R S, Manciu F S, Enriquez J L and Ramana C V 2010 *J. Vac. Sci. Technol. A* **28** 824

[21] Galiote N A, Parreira R L T, Rosolen J M and Huguenin F 2010 *Electrochem. Commun.* **12** 733

[22] Pehlivan E, Niklasson G A, Granqvist C G and Georen P 2010 *Phys. Status. Solidi. A* **207** 1772

[23] Hu M, Wang W D, Zeng J and Qin Y X 2011 *Chin. Phys. B* **20** 102101

[24] Niklasson G A, Malmgren S, Green S and Backholm J 2010 *J. Non-Cryst. Solids* **356** 705

[25] Suvarna R B and Patil P S 2009 *Smart Mater. Struct.* **18** 025004

[26] Liu X B, Ding N F, Jiang A Q and Yang P X 2012 *Appl. Phys. Lett.* **100** 132901

[27] Nah Y C, Ghicov A, Kim D and Schmuki P 2008 *Electrochem. Commun.* **10** 1777

[28] Santato C, Odziemkowski M, Ulmann M and Augustynski J 2001 *J. Am. Chem. Soc.* **123** 10639

[29] Xu Z T, Jin K J, Gu L, Jin Y L, Ge C, Wang C, Guo H Z, Lu H B, Zhao R Q and Yang G Z 2012 *Small* **8** 1279

[30] Karazhanov S Z, Zhang Y, Mascarenhas A, Deb S and Wang L W 2003 *Solid State Ionics* **165** 43

[31] Bohnke O and Robert G 1982 *Solid State Ionics* **6** 115

[32] Niklasson G A, Berggren L and Larsson A L 2004 *Sol. Energy Mater. Sol. Cells* **84** 315

[33] Honig J M 1980 *Electrodes of Conductive Metallic Oxides* (Amsterdam: Elsevier)

[34] Sharma N, Deepa M and Agnihotry S A 2002 *Solid State Ionics* **152** 873

[35] Barsoukov E, Kim J H, Kim J H, Yoon C O and Lee H 1999 *Solid State Ionics* **116** 249